AMERICAN SOCIETY FOR MICROBIOLOGY | Infection and Immunity®

FUNGAL AND PARASITIC INFECTIONS

The Carbohydrate Lectin Receptor Dectin-1 Mediates the Immune Response to *Exserohilum rostratum*

Jennifer L. Reedy,[a,b] Paige E. Negoro,[a] Marianela Feliu,[a] Allison K. Lord,[a] Nida S. Khan,[a] Dan P. Lukason,[a] Nathan P. Wiederhold,[c] Jenny M. Tam,[a,b] Michael K. Mansour,[a,b] Thomas F. Patterson,[c] Jatin M. Vyas[a,b]

Division of Infectious Diseases, Department of Medicine, Massachusetts General Hospital, Boston, Massachusetts, USA[a]; Harvard Medical School, Department of Medicine, Boston, Massachusetts, USA[b]; The University of Texas Health Science Center at San Antonio and South Texas Veterans Health Care System, San Antonio, Texas, USA[c]

ABSTRACT Dematiaceous molds are found ubiquitously in the environment and cause a wide spectrum of human disease, including infections associated with high rates of mortality. Despite this, the mechanism of the innate immune response has been less well studied, although it is key in the clearance of fungal pathogens. Here, we focus on *Exserohilum rostratum*, a dematiaceous mold that caused 753 infections during a multistate outbreak due to injection of contaminated methylprednisolone. We show that macrophages are incapable of phagocytosing *Exserohilum*. Despite a lack of phagocytosis, macrophage production of tumor necrosis factor alpha is triggered by hyphae but not spores and depends upon Dectin-1, a C-type lectin receptor. Dectin-1 is specifically recruited to the macrophage-hyphal interface but not the macrophage-spore interface due to differences in carbohydrate antigen expression between these two fungal forms. Corticosteroid and antifungal therapy perturb this response, resulting in decreased cytokine production. *In vivo* soft tissue infection in wild-type mice demonstrated that *Exserohilum* provokes robust neutrophilic and granulomatous inflammation capable of thwarting fungal growth. However, coadministration of methylprednisolone acetate results in robust hyphal tissue invasion and a significant reduction in immune cell recruitment. Our results suggest that Dectin-1 is crucial for macrophage recognition and the macrophage response to *Exserohilum* and that corticosteroids potently attenuate the immune response to this pathogen.

KEYWORDS Dectin-1, *Exserohilum*, fungi, macrophages, molds

Received 25 October 2016 **Returned for modification** 14 November 2016 **Accepted** 22 December 2016

Accepted manuscript posted online 28 December 2016

Citation Reedy JL, Negoro PE, Feliu M, Lord AK, Khan NS, Lukason DP, Wiederhold NP, Tam JM, Mansour MK, Patterson TF, Vyas JM. 2017. The carbohydrate lectin receptor Dectin-1 mediates the immune response to *Exserohilum rostratum*. Infect Immun 85:e00903-16. https://doi.org/10.1128/IAI.00903-16.

Editor George S. Deepe, University of Cincinnati

Address correspondence to Jatin M. Vyas, jvyas@mgh.harvard.edu.

Dematiaceous molds are melanized, hypha-producing fungi found ubiquitously in the environment. These molds are typically plant pathogens; however, under situations of immunocompromise, allergic disease, or iatrogenic introduction, they are capable of causing disease in humans (1). Dematiaceous molds account for 6 to 10% of invasive fungal infections in solid organ and hematopoietic stem cell transplant recipients (2, 3). Although they represent a small portion of invasive fungal infections, dematiaceous molds are associated with mortality rates ranging from 39 to 72% (2, 3). This diverse group of fungi causes a wide spectrum of human disease, including fungal sinusitis, disseminated infections, pneumonia, and skin and soft tissue infections. In 2012, the dematiaceous mold *Exserohilum rostratum* caused a multistate outbreak due to administration of contaminated methylprednisolone acetate (MPA). To date, 753 clinical infections (including 64 deaths) ranging from meningitis, stroke, and joint infections to local paraspinal infections have been reported (4, 5). The antifungal voriconazole became the treatment of choice for these patients. However, despite

months of antimicrobial therapy, the cessation of voriconazole quickly led to a relapse of infection, indicating the failure of the immune system to clear the infection (6). Only a small subset of drugs within the already limited antifungal armamentarium has reliable activity against dematiaceous molds. In fact, treatment is often a combination of surgical debridement and antifungal therapy, an approach that is limited by the accessibility of the site of infections and the bodily structures involved (7). The triazole antifungals, including voriconazole, are fungicidal against some molds, such as *Aspergillus* species, but against many others they are fungistatic and limit the growth of the fungi, but the host immune system is relied upon for clearance of the organisms. Thus, understanding the rules that govern how the immune system recognizes, responds to, and ultimately clears these pathogens is critical to develop novel treatment strategies, given the unacceptably high mortality rate associated with dematiaceous mold infections.

Macrophages are essential in the recognition and clearance of fungal pathogens; however, most work on the innate immune interaction with fungal pathogens has focused on the most prevalent pathogens, such as *Candida*, *Aspergillus*, and *Cryptococcus* species, with less attention being placed on dematiaceous fungi. To understand fully how the innate immune system combats fungal infections, it is valuable to study a variety of fungal pathogens. Macrophages are present throughout the tissues of the human body and are one of the first immune cells to encounter invading pathogens. Macrophages possess pattern recognition receptors (PRRs) that recognize conserved pathogen-associated molecular patterns (PAMPs) on the surface of pathogens. In fungi, the PAMPs recognized by the innate immune system consist of complex carbohydrates that compose the fungal cell wall (8, 9). PRR activation by PAMPs can result in several outcomes, including phagocytosis and degradation of pathogens, processing of degraded epitopes for loading onto major histocompatibility complex class II molecules, and the release of cytokines that stimulate or dampen the immune response, depending upon the cohort of PRRs engaged (9).

The macrophage response to *Exserohilum* has not previously been defined, despite the important role that macrophages serve in the recognition and response to fungi. Here we characterize the interaction between macrophages and *Exserohilum*, including the PAMPs-PRRs involved in this recognition. We demonstrate that, despite a lack of phagocytosis, macrophages recognize *Exserohilum* and produce potent proinflammatory cytokines. Conidia and hyphae differ in exposed carbohydrate antigens and antigenicity. The PRR C-type lectin Dectin-1 is necessary for the robust production of cytokines and chemokines in response to *Exserohilum* and localizes preferentially to the macrophage-hyphal interface rather than the macrophage-spore interface. Treatment with voriconazole or a corticosteroid alters the production of tumor necrosis factor alpha (TNF-α) by macrophages. Using a soft tissue infection model, we show that the coadministration of methylprednisolone potently enhances the *in vivo* growth and invasion of the pathogen and modulates the immune response.

RESULTS

Macrophages are incapable of phagocytosing *Exserohilum* spores and hyphae. To assess the behavior of macrophages when confronted with *E. rostratum*, we cocultured RAW 264.7 (RAW) macrophages or primary bone marrow-derived macrophages (BMDMs) from C57BL/6 mice with *E. rostratum* spores. Using time-lapse microscopy, we monitored the interactions between *E. rostratum* and macrophages incubated for 18 h. Analysis of the composite videos and individual images demonstrated that macrophages were attracted to *E. rostratum* spores and hyphae but were incapable of phagocytosing the spores and hyphae (Fig. 1A; see Video S1 in the supplemental material). Additionally, the presence of macrophages did not prevent germination of the spores or hyphal elongation. Macrophages showed a preferential attraction to the *E. rostratum* spore poles and hyphae and appeared to cluster less frequently at the middle of the spores. To quantify this interaction, we incubated primary C57BL/6 mouse BMDMs with *E. rostratum* spores overnight, captured differential interference contrast

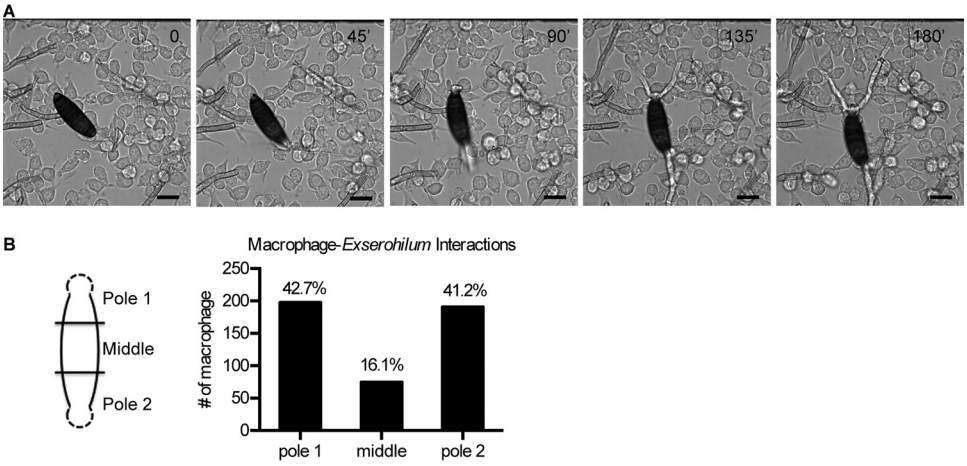

FIG 1 Time-lapse microscopy of *E. rostratum* and macrophages. (A) Purified spores of *E. rostratum* were cocultured with primary C57BL/6 mouse BMDMs or RAW macrophages for 18 h and imaged by time-lapse microscopy. Representative images from coculture with RAW macrophages are shown (the time of image capture [in minutes] is noted in the top right corner). Macrophages failed to phagocytose or inhibit the germination and growth of *Exserohilum* spores. Bars = 20 μm. (B) Quantification of macrophage distribution along the length of the spore. (Left) Spores were divided into three equal compartments on the basis of length. The poles contained the initial hyphal segment (depicted by dashed lines). Pole 1 and pole 2 were randomly assigned to each spore. (Right) The number of macrophages associated with each compartment was counted for 55 spores after 18 h of stimulation. If a spore contacted more than one compartment, it was counted as an interaction for each region. Representative results from a single experiment are shown. A total of 464 macrophage-spore interactions were observed, and the distribution along the spore is depicted. Chi-square tests comparing the expected even distribution (33.3% per compartment) with the observed distribution were performed, and in each experiment (two independent replicates were performed), the results were significantly different from the expected distribution ($P < 0.001$) and skewed toward an increased interaction between macrophages and spore poles.

(DIC) images of 50 to 100 individual spores of *E. rostratum*, divided the germinated spore into three sections of equal length (Fig. 1B), and counted the number of macrophages contacting the spore in each compartment. We compared the average number of macrophages per compartment with the number that would be expected on the basis of an equal distribution. In each case, there was a significant deviation ($P < 0.001$) of the observed from the expected results (a random distribution would generate 33.3% of the interactions in each segment), with a higher percentage of interactions occurring at the poles rather than at the center of spores (Fig. 1B).

Fungal cell wall carbohydrate antigens differ between spores and hyphae. The preferential clustering of macrophages around hyphae and spore poles rather than spore bodies suggested that these structures differ in their antigenicity. Based upon this different attraction, we hypothesized that the surface exposure of carbohydrate antigens differs between spores and hyphae. *Aspergillus fumigatus* and *Cryptococcus neoformans* spores are known to differ in cell wall composition and structure from the hyphal and yeast growth forms, respectively (10–14). The fungal cell wall is a carbohydrate-rich structure typically composed of chitin, β-glucans, and mannans. However, there is variability between species with respect to the components of the fungal cell wall, the structural characteristics of the carbohydrates, and the accessibility of specific carbohydrates. For instance, *Cryptococcus* elaborates a dense polysaccharide capsule, which shields cell wall carbohydrates from detection by the immune system (15, 16). As cell wall carbohydrates are the primary PAMPs in fungal pathogens, we focused our analysis on carbohydrates that are known or suspected to provoke an immune response in other fungal species, including mannan (17–20), β-1,3-glucan (21–30), galactosaminogalactan (GAG) (31–36), and chitin (37–45). Freshly harvested *Exserohilum rostratum* spores were grown in complete RPMI at 37°C with 5% CO_2. These growth conditions were chosen since they are the identical conditions under which coculture experiments with *E. rostratum* and macrophages were performed; thus, the carbohydrate expression profiles observed should be similar to those displayed in the presence of macrophages in stimulation experiments. *E. rostratum* spores were incu-

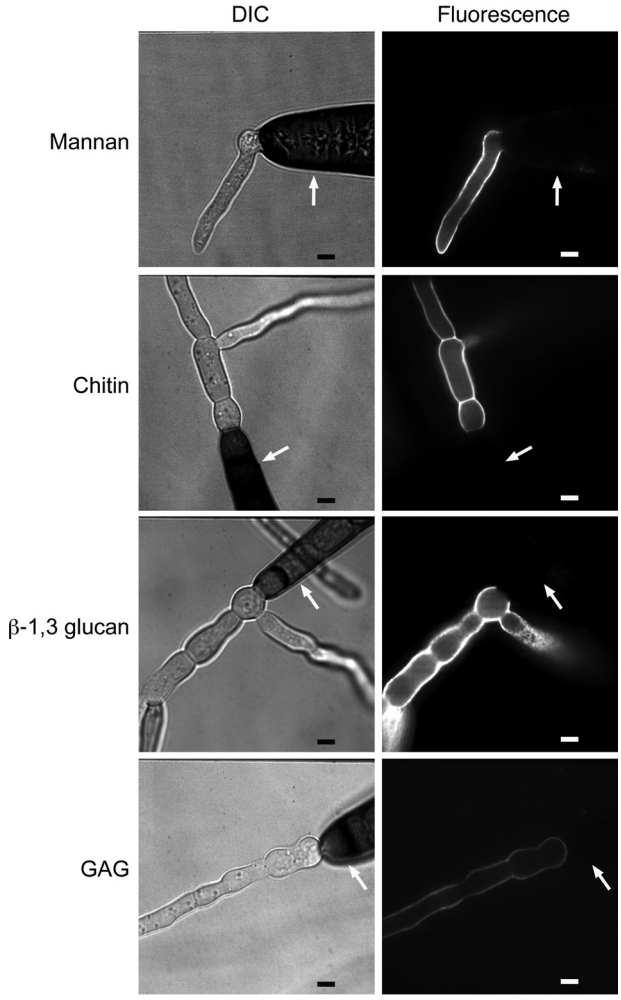

FIG 2 Carbohydrate antigens differ between *E. rostratum* spores and hyphae. Spores were germinated in complete RPMI for 5 h (mannan and GAG) or 18 h (β-1,3-glucan and chitin). Cells were stained with calcofluor white (chitin stain), fluorescein-conjugated concanavalin A (mannan stain), anti-β-1,3-glucan with secondary anti-mouse IgG conjugated with Alexa Fluor 488 (β-1,3-glucan stain), and fluorescein-conjugated soybean agglutinin (GAG stain) and imaged via confocal microscopy using DIC and fluorescent imaging. All lectins and antibodies shown preferentially labeled the hyphae but not the spores of *Exserohilum*. White arrows pointing to spore bodies highlight the lack of staining. Bars = 5 μm.

bated for various lengths of time (0, 4, 6, 8, 18 h) and then stained to visualize surface carbohydrates. Spores that had not yet germinated (time zero) did not stain for any of the carbohydrates tested (data not shown). We chose 4 h as the minimum time that the spores were accessed after inoculation into RPMI 1640 medium (RPMI) since at that time nearly all spores had germinated. In sharp contrast to conidia, hyphae demonstrated abundant mannan, chitin, β-1,3-glucan, and GAG, as demonstrated by fluorescence-based imaging (Fig. 2). The staining pattern of hyphae and spore bodies remained stable at all time points tested postgermination. The differential exposure of antigens on hyphae compared with that on spores indicates that the antigenicity of the spores and hyphae differs and accounts for the preferential attraction of macrophages to hyphae demonstrated by time-lapse microscopy.

TNF-α production by macrophages requires *E. rostratum* hyphal growth. Since macrophages are attracted to *E. rostratum* hyphae, which contain proinflammatory antigens, such as β-1,3-glucan, we hypothesized that macrophages produce proinflammatory cytokines, such as TNF-α, in the presence of *E. rostratum*. To test this hypothesis, we stimulated wild-type (WT) C57BL/6 mouse BMDMs with *E. rostratum* spores for 18 h. By this time, all the spores had germinated and formed extensive hyphal networks.

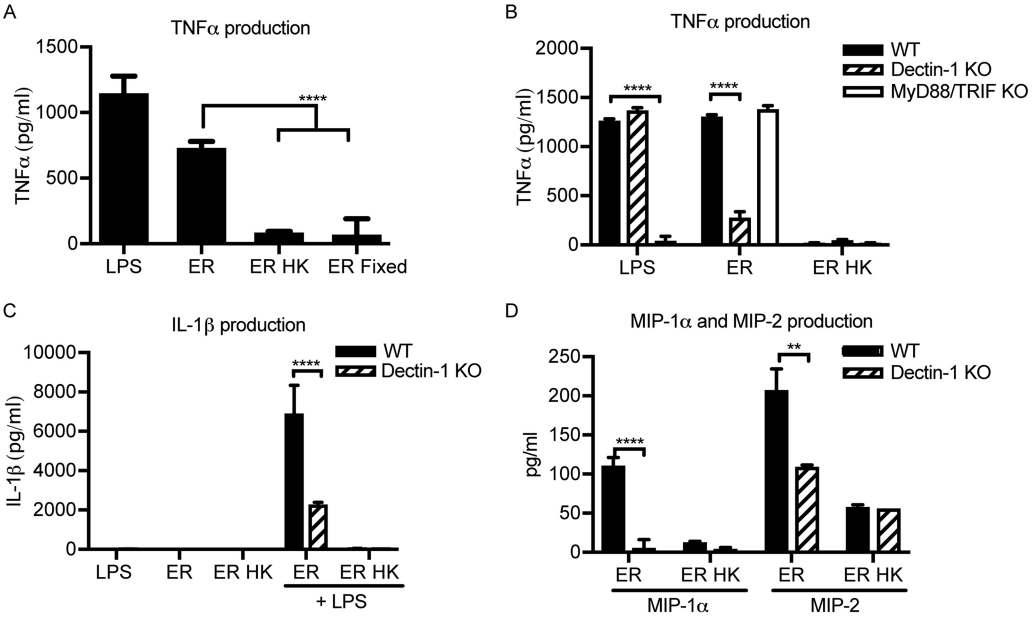

FIG 3 TNF-α production by macrophages exposed to *E. rostratum* requires hyphae and Dectin-1. Macrophages were stimulated for 18 h with *E. rostratum* at an MOI of 1:50. (A) C57BL/6 BMDMs were stimulated with live *E. rostratum* spores (ER), heat-killed *E. rostratum* spores (ER HK), or paraformaldehyde-fixed *E. rostratum* spores (ER Fixed). LPS was used as a positive control for TNF-α production. Live spores were capable of germination and produced robust hyphae by 18 h. Heat-killed and fixed spores were killed and thus did not germinate. Macrophages that were stimulated with live spores with hyphal formation had increased levels of TNF-α production compared with macrophages stimulated with spores incapable of germinating (heat killed and fixed), ($P < 0.0001$). (B) *Exserohilum* spores (live or heat killed) were cocultured with BMDMs from wild-type C57BL/6 mice (WT), Dectin-1 knockout mice, or MyD88/TRIF knockout mice. The level of production of TNF-α in response to live spores was significantly lower for Dectin-1 KO BMDMs than WT BMDMs ($P < 0.0001$). However, there was no significant difference in the levels of TNF-α production between WT and MyD88/TRIF BMDMs. (C) Macrophages were stimulated with LPS, *E. rostratum* conidia, or heat-killed *E. rostratum* conidia or were first prestimulated with LPS for 4 h prior to stimulation with *E. rostratum* conidia and heat-killed *E. rostratum* conidia. IL-1β was produced in response to *E. rostratum* after prestimulation with LPS, and its level was significantly decreased in the Dectin-1 KO BMDMs ($P < 0.0001$). (D) WT and Dectin-1 KO BMDMs were stimulated with *E. rostratum* and heat-killed *E. rostratum*. The levels of production of both MIP-1α and MIP-2 were significantly reduced in Dectin-1 KO macrophages ($P < 0.0001$ and $P \leq 0.01$, respectively). The data represent the means and SEMs from 3 biological replicates performed for each treatment condition (three independent experiments were performed with similar results). Significance was calculated using ANOVA with the Tukey posttest (A) and two-way ANOVA (B, C, D). **, $P \leq 0.01$; ****, $P < 0.0001$.

The results demonstrate that TNF-α is produced in response to *E. rostratum*, despite the inability of the macrophages to phagocytose the spores and hyphae (Fig. 3A). Given the differential display of carbohydrate antigens between spores and hyphae revealed through staining, we predicted that there may be an increased cytokine response to *E. rostratum* hyphae compared with that to spores. To test this hypothesis, we stimulated C57BL/6 mouse BMDMs with live *E. rostratum* conidia (which are capable of germinating and forming hyphae within 4 h of coincubation) or killed conidia (without hyphae). Since prior studies have demonstrated that heat killing can alter the carbohydrate structure of yeast by stripping off the mannan layer and increasing the level of exposure of β-1,3-glucans (19, 46–48), we chose two different methods of killing (e.g., heat and paraformaldehyde fixation), as it was less likely that both methods would produce the exact same changes to the carbohydrate composition of the spores. Additionally, heat-killed spores did not stain positive for any of the carbohydrates tested previously, including β-1,3-glucan, similar to the findings for live but ungerminated spores (data not shown). After 18 h of coincubation, we measured the TNF-α concentration in the supernatants. There was a significantly lower level of production of TNF-α in response to heat-killed or fixed spores compared with that in response to germinated conidia, demonstrating that the presence of hyphae is important for generating a robust proinflammatory response (Fig. 3A).

The carbohydrate lectin receptor Dectin-1 is necessary for cytokine and chemokine production. We examined the role of known pattern recognition recep-

tors (PRRs) in mediating macrophage recognition and response to *E. rostratum*. Several classes of PRRs mediate macrophage binding of fungal PAMPs, including C-type lectin receptors (CLRs) and Toll-like receptors (TLRs). Recognition of fungal PAMPs by their cognate PRRs results in the induction of downstream signaling events, including induction of phagocytosis and production of cytokines and chemokines. We hypothesized that Dectin-1, a C-type lectin receptor that recognizes β-1,3-glucan (47, 49–51), may play a critical role in the cytokine and chemokine response to *E. rostratum*, given the presence of β-1,3-glucan on the surface of *E. rostratum* hyphae. Dectin-1 mediates the recognition of multiple fungal pathogens independently and in association with TLR2 and TLR4 (52–54). TLR2, TLR4, and TLR9 also recognize the fungal pathogens *Candida albicans* and *A. fumigatus* (46, 55–57). To determine the roles that Dectin-1 and TLRs play in the response to this fungal pathogen, we utilized primary BMDMs from wild-type C57BL/6 mice, Dectin-1 knockout (KO) mice, and MyD88/TRIF knockout mice. The MyD88/TRIF adaptor proteins function downstream of TLRs; thus, a double-knockout strain behaves as a TLR signaling-deficient strain (58). We stimulated macrophages with *E. rostratum* conidia for 18 h and measured the TNF-α responses. There was not a significant change in the TNF-α response between wild-type and TLR signaling-deficient macrophages (Fig. 3B), indicating that TLR-dependent signaling was dispensable for TNF-α production. However, there was a significant decrease in the level of TNF-α production in Dectin-1-deficient macrophages (Fig. 3B). To elucidate further the role of Dectin-1 in cytokine and chemokine production in response to *E. rostratum*, we assessed the production of interleukin-1β (IL-1β), a proinflammatory cytokine produced via inflammasome activation (59, 60), and the chemokines macrophage inflammatory protein 1 alpha (MIP-1α) and macrophage inflammatory protein 2 (MIP-2), which mediate neutrophil recruitment. These signaling molecules are produced in response to the fungal pathogen *Aspergillus fumigatus* in a Dectin-1-dependent manner (61). IL-1β was produced in response to live *E. rostratum* when macrophages were prestimulated with lipopolysaccharide (LPS) and was significantly decreased in the Dectin-1-deficient cells (Fig. 3C). Similarly, Dectin-1 knockout BMDMs produced significantly less MIP-1α and MIP-2 than wild-type BMDMs (Fig. 3D). Heat-killed *E. rostratum* spores induced less IL-1β, MIP-1α, and MIP-2 than live *E. rostratum* conidia, further demonstrating the role of hyphae in the generation of cytokines and chemokines. In control experiments, wild-type and Dectin-1 knockout BMDMs were stimulated with LPS plus ATP (IL-1β) or LPS alone (MIP-1α and MIP-2), and it was demonstrated that Dectin-1 deficiency did not impair the response to these stimuli (data not shown). These results demonstrate that Dectin-1 plays a key role in generating a cytokine and chemokine response to *Exserohilum*.

Dectin-1 is concentrated at sites of macrophage-hyphal interactions but not macrophage-spore interactions. Given that exposure of β-1,3-glucan differs between spores and hyphae, we hypothesized that Dectin-1 would preferentially localize to sites of macrophage-hyphal interactions but not macrophage-spore interactions. To assess this hypothesis, we utilized macrophages that express a green fluorescent protein (GFP)–Dectin-1 (GD1) fusion protein (62). We stimulated GD1-expressing macrophages with *E. rostratum* for either 4 or 18 h. We performed live cell imaging of samples stained with calcofluor white (chitin stain) (Fig. 4B) or fixed the samples and immunostained them for β-1,3-glucan to visualize *E. rostratum* hyphae (Fig. 4A). We then imaged the cells using confocal microscopy. These studies revealed that Dectin-1 localized to the macrophage-hyphal interface but not the macrophage-spore interface. Dectin-1 strongly localized in a ring formation to the site of initial hyphal extrusion from the spore. This localization may be secondary to a unique feature of the *E. rostratum* cell wall at this junction, or this is simply the first area that hyphal wall carbohydrates become accessible to macrophages and, hence, Dectin-1 strongly localizes to this area. Interestingly, macrophages that are in contact with *E. rostratum* hyphae show weak Dectin-1 recruitment along the remainder of their membrane by 18 h, indicating that the majority of the Dectin-1 protein has become polarized to the macrophage-hyphal contact region. Macrophages that are in the same well but not in contact with *E.*

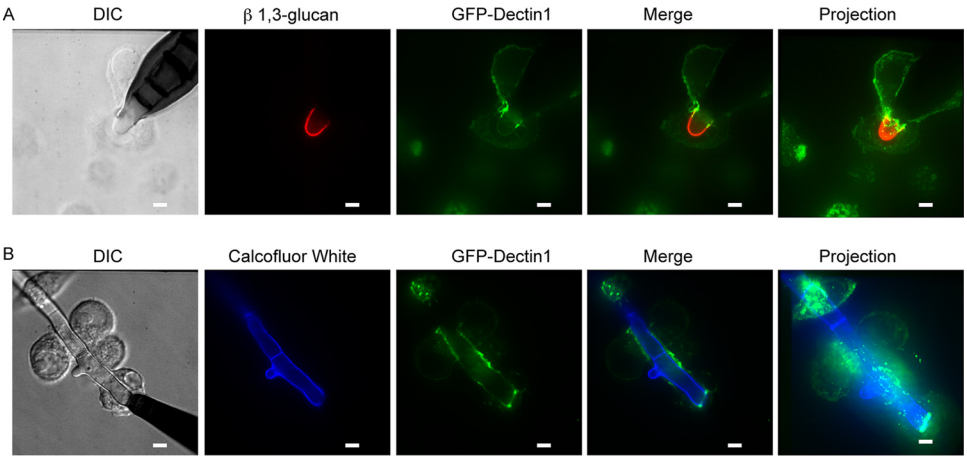

FIG 4 Dectin-1 is recruited to *Exserohilum* hyphae but not spores. *Exserohilum* spores were coincubated with GFP–Dectin-1-expressing RAW macrophages for 6 h (A) or 18 h (B). (A) Samples were fixed, permeabilized, and stained with anti-β-1,3-glucan and secondary anti-mouse IgG conjugated to Alexa Fluor 488 to visualize β-1,3-glucan on the *Exserohilum* surface. Labeled samples were imaged by confocal microscopy. Projection images are reconstructions created from z-stack images. Dectin-1 localized most intensely at points of macrophage-hyphal interaction and particularly at the base of the hyphae. (B) Cocultured live cells were stained with calcofluor white and imaged by confocal microscopy. Dectin-1 again localized at areas of macrophage-hyphal interaction and particularly at the base of the hyphae. There was little recruitment to areas of macrophage-spore interaction. Representative images are shown. All experiments were performed in triplicate. Bars = 5 μm.

rostratum show a uniform intensity of GFP fluorescence on their membrane surface (data not shown). Dectin-1 is highly recruited to the area of hyphal contact over time and appears to be driven to the cell membrane in direct contact with hyphae.

Treatment with voriconazole or corticosteroid diminishes TNF-α production, but only voriconazole decreases hyphal growth. We were interested in how the exposure to antifungals and corticosteroids impacts the macrophage-*Exserohilum* interactions. These compounds were administered to patients infected with *Exserohilum* during the outbreak and are commonly administered to patients with fungal infections. Immunosuppression with high-dose corticosteroids is an established risk factor for the development of invasive fungal infections, although the mechanism of action has not been fully elucidated. Voriconazole was the recommended antifungal therapy for patients with *Exserohilum* meningitis (63, 64) and is a common therapeutic agent used against dematiaceous mold infections. Thus, understanding how these drugs affect macrophage-fungus interactions has important clinical consequences. Despite several months of voriconazole therapy, relapsed infection has occurred (6), suggesting that antifungal therapy alone is not sufficient for the clearance of these pathogens and that concurrent immune clearance is essential. Given that voriconazole works by disrupting the biosynthesis of cell membrane ergosterol, we hypothesized that voriconazole therapy may alter macrophage-*Exserohilum* interactions. Carbohydrate staining of the fungal surface did not reveal significant alterations in carbohydrate staining with either voriconazole or the corticosteroid methylprednisolone succinate (MPS) (data not shown). We chose to use methylprednisolone, as this is the corticosteroid that was contaminated by *E. rostratum* during the outbreak. For the *in vitro* experiments we used MPS, the succinate form, as it is a clear liquid and, thus, does not interfere with microscopy or fluorescence measurements. To determine the effect of voriconazole and corticosteroid treatment on cytokine production in response to *E. rostratum*, we stimulated macrophages with *E. rostratum* in complete RPMI with or without 1, 5, or 50 μg/ml voriconazole or 50 μg/ml MPS for 18 h, at which time TNF-α concentrations were measured. We chose a range of voriconazole concentrations based upon published MIC ranges for *Exserohilum* clinical isolates (MIC range, $<$0.03 to 1 μg/ml) (65). Treatment of *E. rostratum* with voriconazole did not prevent spore germination at any of the dosages tested but did result in morphologically aberrant hyphae that were shorter in length and had increased proximal branching compared with untreated hyphae (Fig. 5A).

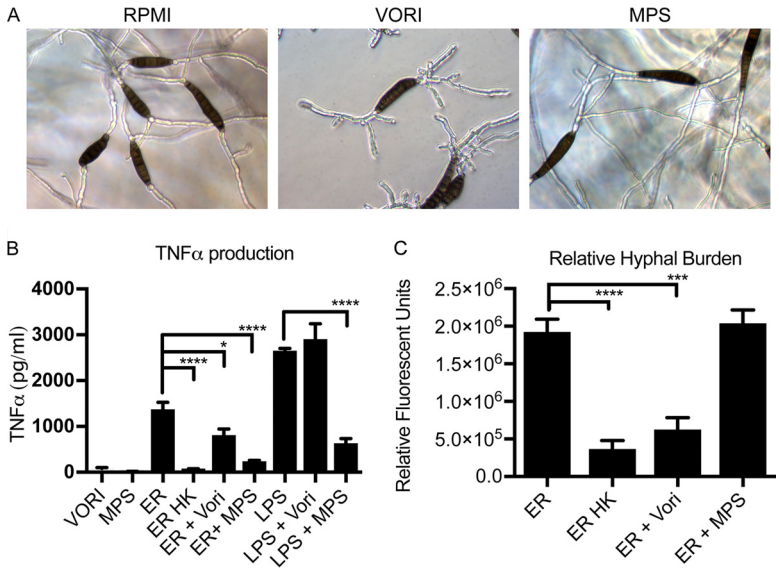

FIG 5 Treatment with voriconazole or corticosteroid decreases cytokine production, but only voriconazole alters the hyphal burden. (A) *E. rostratum* spores were grown in complete RPMI alone or complete RPMI with 50 μg/ml MPS or 50 μg/ml voriconazole (VORI). Spores incubated for 18 h in RPMI alone and complete RPMI with MPS exhibited similar hyphal growth with long hyphae. However, spores grown in RPMI with voriconazole were capable of germinating but formed markedly aberrant hyphae with short, frequent branches and decreased lengths. (B) *Exserohilum* spores were cocultured with primary C57BL/6 mouse BMDMs for 18 h in the presence or absence of MPS or voriconazole. TNF-α production was measured and found to be decreased in both the corticosteroid-treated and voriconazole-treated samples. Macrophages stimulated with MPS or voriconazole alone had the background level of TNF-α production. (C) The hyphal burden at 18 h was quantified by staining samples with calcofluor white and measuring the fluorescence. Fluorescence is reported as relative fluorescence, which is the number of fluorescent units above that for the background control. There was a significantly lower hyphal burden in voriconazole-treated samples. The presence of some fluorescence in the heat-killed sample is likely secondary to the presence of small hyphal fragments retained in the spore preparations. Significance was calculated using ANOVA with Tukey posttests. *, $P \leq 0.05$; ***, $P \leq 0.001$; ****, $P < 0.0001$.

Treatment with MPS did not grossly alter the hyphal morphology (Fig. 5A). Addition of voriconazole resulted in slightly decreased levels of cytokine production in response to *E. rostratum* (Fig. 5B), while treatment with MPS resulted in a robust decrease in the levels of cytokine production in response to both *E. rostratum* and LPS (Fig. 5B). We hypothesized that the decreased level of cytokine production in response to voriconazole could be due to the decreased hyphal length of *E. rostratum* grown in the presence of voriconazole. To measure hyphal mass changes between untreated and voriconazole-treated samples, we utilized calcofluor white staining. Calcofluor white binds chitin and preferentially binds *E. rostratum* hyphae but not spores. Since the entire length of the hyphae is stained by calcofluor, the volume of hyphae in a sample correlates with the calcofluor fluorescence. This technique has been used to measure hyphal mass in *A. fumigatus* (66), since other methods, such as determination of the number of colony-forming units (CFU) and the optical density at 600 nm, can have technical limitations due to the hyphal growth form of these organisms. Staining with calcofluor white revealed that there was a decreased hyphal volume when fungi were treated with voriconazole (Fig. 5C). We also measured the hyphal volume in the presence of MPS and found that growth was similar in the presence and absence of MPS.

Given that Dectin-1 is critical for cytokine production with β-1,3-glucan-containing pathogens, we examined whether treatment with a corticosteroid or voriconazole would alter Dectin-1 recruitment to the site of macrophage-hyphal interactions. We stimulated GD1-expressing macrophages with *E. rostratum* in complete RPMI alone or RPMI containing 50 μg/ml of either voriconazole or MPS and at 18 h fixed the cultures and visualized β-1,3-glucan using immunofluorescence. Under all treatment conditions,

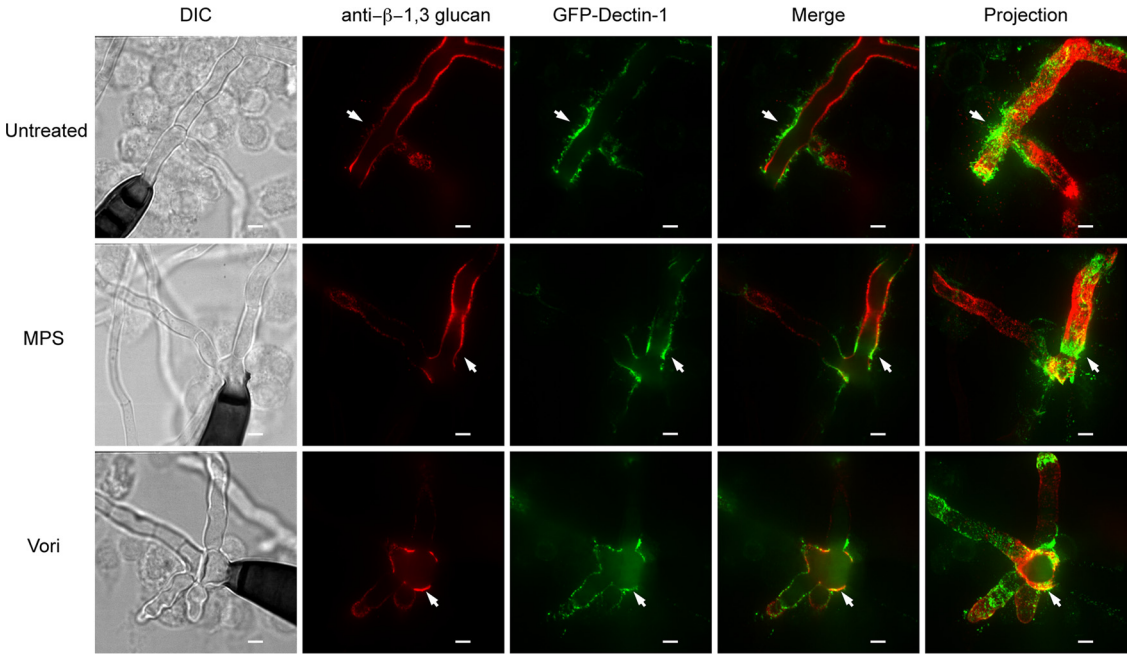

FIG 6 Treatment with voriconazole or corticosteroids does not alter GFP–Dectin-1 recruitment to hyphae. *Exserohilum* spores and GFP–Dectin-1-expressing RAW macrophages were incubated for 18 h in complete RPMI alone or complete RPMI with MPS at 50 μg/ml or voriconazole (Vori) at 50 μg/ml. Under all treatment conditions, GFP–Dectin-1 localized to points of macrophage-hyphal interaction, highlighted by white arrows. There was no GFP–Dectin-1 localization to macrophage-spore interactions. Bars = 5 μm.

Dectin-1 was still recruited to the macrophage-hyphal interface, and there was no significant difference in β-1,3-glucan expression on hyphal surfaces. Therefore, alterations in cytokine production did not appear to result from the failure of Dectin-1 recruitment (Fig. 6) or β-1,3-glucan expression. These observations support the hypothesis that the decrease in the TNF-α response to *Exserohilum* treated with voriconazole is secondary to the decreased hyphal mass. While MPS globally reduced the production of proinflammatory TNF-α in response to pathogenic stimuli, including the control LPS stimulus and *Exserohilum*, the decreased cytokine response to *Exserohilum* in the presence of voriconazole was unique to *Exserohilum* and likely secondary to reduced growth. These results demonstrate that alterations in fungal growth as a result of antifungal therapy with voriconazole can affect macrophage-fungus interactions and result in decreased proinflammatory TNF-α signaling.

Corticosteroid treatment results in an increased hyphal burden and decreased recruitment of immune cells to sites of infection *in vivo*. Previous work with *E. rostratum* demonstrated that heterologous hosts, such as *Drosophila melanogaster*, could be used to model infection (67). We were interested in developing a mammalian soft tissue model of infection that could be used to evaluate the role of defined immunological defects in susceptibility to *Exserohilum* and the role of treatments such as corticosteroids. We developed a soft tissue model of infection in mice, since the *Exserohilum* infections were secondary to inoculation of contaminated methylprednisolone acetate (MPA) into the joints of patients with extension into soft tissue. Additionally, a review of all published infections secondary to *Exserohilum* infection prior to 2012 showed that skin (cutaneous and subcutaneous) infections were the second most frequent manifestation of infection (the most common was systemic disease) (68). For our model, we shaved the posterior flanks/thighs of the mice and injected 2×10^5 spores in 120 μl of phosphate-buffered saline (PBS)–0.008% Tween. For all mice, the right upper thigh was injected with the vehicle control and the left upper thigh was injected with *Exserohilum*. The infection was allowed to persist for 10 days, at which point the mice were euthanized and soft tissue was excised for histological examination. External measurements of the area of induration were taken

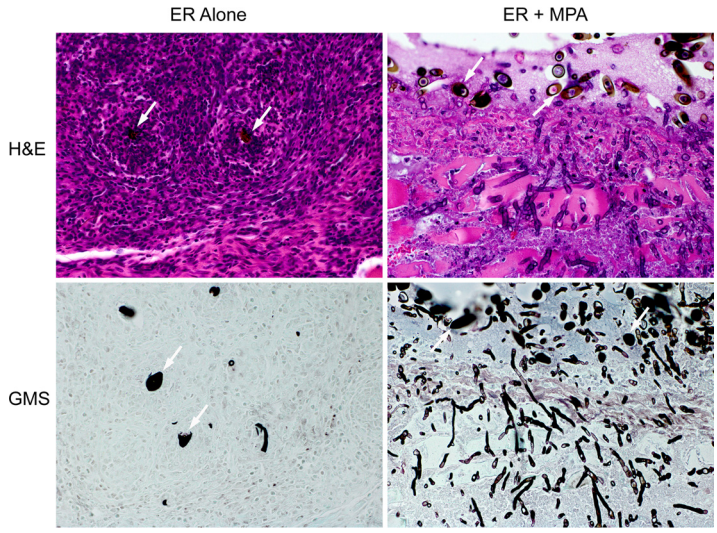

FIG 7 Soft tissue infection model. *Exserohilum* spores (2×10^5) were injected into the right thigh of WT C57BL/6 mice and Dectin-1 knockout mice in PBS–0.008% Tween or PBS–0.008% Tween containing 13 mg/ml of methylprednisolone acetate. Mice were sacrificed on day 10, and tissue was fixed and stained with H&E and GMS. Dectin-1 knockout mice and wild-type mice had similar inflammatory and fungal growth patterns. Images are ×400 magnifications of tissue at the site of *Exserohilum* spore injection and are from Dectin-1 knockout mice. White arrows, spores seen in a tissue section. Injection of *Exserohilum* alone was characterized by cellular infiltrates with multinuclear giant cells and granuloma formation consisting of neutrophils and histiocytes around spores. There was little to no hyphal growth on GMS staining. Injection of *Exserohilum* with corticosteroids resulted in a significant decrease in inflammatory cell recruitment and robust hyphal formation. Invasion of hyphae into surrounding muscle is shown in both the H&E- and GMS-stained images.

using digital calipers; however, the differences between the treatment groups were not statistically significant. No induration was seen at the site of the control injections by 10 days. Samples were stained with hematoxylin and eosin (H&E) and modified Grocott's methenamine silver (GMS) and reviewed by the Massachusetts General Hospital (MGH) Histopathology Research Core. Given that our *in vitro* data indicated a role for Dectin-1 in the macrophage response to *E. rostratum*, we first compared the responses of Dectin-1 KO and WT C57BL/6 mice. Both Dectin-1 KO and wild-type mice showed a similar inflammatory response with predominately neutrophilic infiltration and the formation of granulomas (Fig. 7). There were numerous multinuclear giant cells within the involved area. Little to no hyphal growth was observed on sections stained with GMS (Fig. 7). We also evaluated the effects of the coinoculation of the corticosteroid MPA and *E. rostratum* in both murine strains. For our *in vivo* model, we chose to use the acetate formulation of methylprednisolone to more closely mimic the iatrogenic introduction during the *E. rostratum* outbreak. MPA is a cloudy suspension of methylprednisolone but, unlike MPS, stays at the site of injection with less systemic spread, thus creating local but not global immunosuppression. In these experiments, mice were injected with PBS-Tween with 13 mg/ml MPA. We chose the coinjection of MPA with the *Exserohilum* sample since this local immunosuppression rather than global immunosuppression of the mice more closely modeled the outbreak scenario. Coadministration of MPA and *E. rostratum* resulted in a significantly decreased recruitment of neutrophils, particularly at the site of initial inoculum deposition (visible in tissue, due to the presence of spores). Unlike the findings for mice that received *Exserohilum* alone, no granulomas were seen at the site of spore deposition, there was a significant increase in hyphal growth with penetration into the surrounding muscle (Fig. 7), and in one case, there was the formation of a skin ulceration. A previously published review of the histopathology from 40 cases of *Exserohilum* human infections (69) showed a predominately necrosuppurative and granulomatous inflammation, similar to the types of inflammation noted in our experimental model of *Exserohilum*.

Our results indicate that MPA potently modulates the recruitment of innate immune cells (e.g., neutrophils) to the site of infection, permitting unchecked hyphal growth and deeper tissue invasion.

DISCUSSION

Given the importance of the innate immune system in the recognition and clearance of fungal pathogens, we undertook this study to understand how macrophages recognize and respond to *E. rostratum*. This study is the first exploration of the role that macrophages and Dectin-1 play in the recognition and response to this fungal pathogen. Our work demonstrated that macrophages are incapable of phagocytosing *Exserohilum* but still mount a Dectin-1-dependent cytokine and chemokine response in response to *E. rostratum* hyphae.

We demonstrated that macrophages show a preferential localization to hyphae and the poles of spores rather than spore bodies. Carbohydrate analysis revealed that there is differential exposure of carbohydrate antigens between spores and hyphae. Hyphae express a variety of immunomodulatory carbohydrates, whereas spore carbohydrates, if present, were inaccessible for staining. The ability of antibodies and lectins to bind cell wall carbohydrate suggests that these epitopes are accessible for immune recognition, with the exception of accessibility by calcofluor white (chitin stain), which is a small molecule and is thought to be a less reliable indicator of carbohydrate accessibility. The lack of spore staining suggests either that these carbohydrates are not being produced as part of the spore cell wall or that the carbohydrate layer is being masked. The pigmentation of *Exserohilum* suggests that it contains melanin in the cell wall, similar to other pigmented yeasts and molds. It is possible that melanin or a protein is masking the detection of carbohydrates in the spores. For example, *A. fumigatus* spores are coated with the RodA hydrophobin, which alters the surface hydrophobicity of spores and also alters their immunogenicity by masking carbohydrates (10). It is possible that a similar phenomenon may be occurring in *Exserohilum*. Additionally, carbohydrate components such as α-1,3-glucans can conceal the underlying β-1,3-glucan layer from innate immune detection (70). The difference in carbohydrate exposure on the surface of *Exserohilum* contributes to the preferential attraction of macrophages to hyphae rather than spore bodies.

In support of the hypothesis that macrophages respond differently to spores and hyphae, we demonstrated that *Exserohilum* hyphae induce a more robust TNF-α response than spores alone. In addition, Dectin-1 is highly localized to the sites of macrophage-hyphal interactions but not sites of macrophage-spore interactions. We hypothesize that cytokine production in wild-type macrophages is the result of frustrated phagocytosis, a process that occurs when macrophages are stimulated by but are unable to phagocytose large particles. Dectin-1 activation has been shown to mediate enhanced cytokine production during the process of frustrated phagocytosis with large insoluble particles of β-1,3-glucan (71, 72). Furthermore, internalization of Dectin-1 is required for turning off signaling (71, 72) and, likely, recycling of the receptor. This observation may explain the significant decrease in cytokine production when Dectin-1 is absent. It is interesting to note that after 18 h of coincubation there was a profound imbalance in the distribution of Dectin-1 within macrophage-contacting hyphae, with robust GFP localization being seen at the macrophage-hyphal interface and very low levels of GFP being seen around the remainder of the cell membrane. This imbalance was not seen in cells that were in the same wells but not in contact with *Exserohilum*. This raises the possibility that there may be continual recruitment of the cellular pool of Dectin-1 to the area of the macrophage-hyphal interaction, given the lack of phagocytosis and, possibly, alterations in recycling of the Dectin-1 protein.

In the 2012 fungal meningitis outbreak, *Exserohilum* was inoculated into patients through injection of contaminated corticosteroids (4). Previous work demonstrated that *Exserohilum* has an enhanced rate of growth in the presence of corticosteroids (67). It should be noted that the concentration used in our *in vitro* experiments, 50 μg/ml, was

one that did not produce a significantly enhanced growth pattern in the previous study (67). We demonstrated that corticosteroid treatment significantly reduced the level of production of TNF-α in response to *Exserohilum* but also in response to LPS, suggesting that the signaling defect is not specific to *Exserohilum* but is a more global defect in cytokine signaling responses. As Dectin-1 is still recruited to the macrophage-hyphal interface, these data suggest that the signaling blockade is downstream of Dectin-1. Since voriconazole was the treatment of choice during the *Exserohilum* outbreak and is a commonly used antifungal in the treatment of dematiaceous mold infections in general, we were interested in the effect of voriconazole therapy on macrophage-*Exserohilum* interactions. We demonstrated that voriconazole did not prevent the germination of spores but did result in marked aberrations in growth and truncated hyphae. There was also a significant decrease in the level of cytokine production in response to *Exserohilum* in the presence of voriconazole. We hypothesized that this may be secondary to the reduced hyphal burden in culture. In both corticosteroid and voriconazole treatment, Dectin-1 was still recruited to the site of macrophage-hyphal interactions, suggesting that defects in cytokine production were not the result of an alteration in the accessibility of β-1,3-glucan or the recruitment of Dectin-1. The decreased proinflammatory TNF-α response in the presence of voriconazole demonstrates that antifungal treatment of fungal pathogens can modulate how the host responds to the fungus and may serve as a mechanistic explanation of why relapse occurs after the cessation of antifungal therapy in patients.

We also developed a murine soft tissue model of infection that enabled us to test the *in vivo* role of Dectin-1 deficiency and corticosteroid treatment. Wild-type mice inoculated with *Exserohilum* demonstrated predominately neutrophilic infiltrates with granulomatous inflammation, multinuclear giant cells, and rare hyphal growth. The types of inflammatory response seen in our model mirrored the inflammatory responses seen in an analysis of 40 patients infected with *Exserohilum* during the clinical outbreak (69). The correlation between the histology seen in our murine *in vivo* model and that seen in patients suggests that this may be a robust model for studying dematiaceous mold infections. Despite the *in vitro* importance of Dectin-1 in mediating cytokine expression, there was no difference in the type of inflammatory response and fungal control between wild-type and Dectin-1-deficient mice. However, coadministration of *Exserohilum* and corticosteroids markedly altered the inflammatory response and greatly enhanced the fungal tissue burden.

Our *in vitro* work demonstrated that Dectin-1 mediates macrophage recognition of *E. rostratum* and the production of cytokines and chemokines, although we did not observe any significant differences in histology between wild-type and Dectin-1-deficient mice in our *in vivo* model. There are several possible explanations for this finding. First, we limited our analysis to histopathology, although analysis of the cytokine responses *in vivo* may have revealed differences. Second, although Dectin-1-deficient macrophages have decreased levels of TNF-α, IL-1β, MIP-1α, and MIP-2 production, the amount produced may be sufficient for immune activation. Third, there may be Dectin-1-independent pathways including complement (all of the *in vivo* experiments were performed under conditions with depletion of active complement) that could overcome defects in macrophage responses. Lastly, there are additional immune effector cells, such as dendritic cells and neutrophils, in the *in vivo* milieu that may generate a response to *Exserohilum* in a Dectin-1-independent manner utilizing alternative CLRs, such as DC-SIGN or Dectin-2/3 (73, 74). A deficiency of caspase recruitment domain-containing protein 9 (Card9) increased susceptibility to the dematiaceous mold *Phialophora verrucosa* (75, 76). Card9 mediates signaling from multiple C-type lectin receptors, including Dectin-1, suggesting a role for CLRs in response to dematiaceous mold infections. Histology from WT and Dectin-1$^{-/-}$ mice treated with *Exserohilum* demonstrated spores surrounded by granulomatous inflammation but little to no hyphal formation. As our *in vitro* results demonstrated that hyphae promote more robust Dectin-1-dependent TNF-α production than spores, the paucity of visible hyphae may suggest that *in vivo* signaling is driven by alternative pathways. The

histological examination, however, is not sensitive enough to demonstrate whether there was initiation of hyphal formation or, possibly, early small hyphal formation that played a role in triggering the inflammatory response.

The coadministration of *Exserohilum* with corticosteroids resulted in decreased immune cell recruitment to the site of initial infections and robust hyphal growth. As the distance from the site of initial inoculum deposition increased, there was increased neutrophil recruitment, possibly secondary to a decrease in the corticosteroid concentration with distance; however, no granuloma formation was seen. The increased growth of the *Exserohilum* with corticosteroid is likely multifactorial. First, the coadministration of *Exserohilum* and high levels of MPA may enhance fungal growth (67), since the concentration used in this experiment was higher than that used in our *in vitro* studies to reflect patient exposure. Second, our *in vitro* work shows that corticosteroids significantly reduce the level of production of TNF-α by macrophages, which may influence the recruitment of additional immune cells to the site of infection. Third, methylprednisolone decreases the phagocytic activity of neutrophils toward *Exserohilum* (77). All of these factors may contribute to the lack of immune cell recruitment at the initial site of infection and the enhanced hyphal growth in tissue. This model shows that the combination of *Exserohilum* with corticosteroids provided an optimal milieu for invasion and establishment of clinical disease.

In conclusion, our results show that macrophages recognize and signal in response to *Exserohilum* hyphae in a Dectin-1-dependent manner even in the absence of phagocytosis. Treatment with corticosteroids perturbs the ability of macrophages to produce TNF-α and significantly enhances the ability of *Exserohilum* to establish infection. The vertebrate *in vivo* model could be extended to other dematiaceous molds and filamentous fungi and help elucidate the impact of defined immunodeficiencies and drug therapies on the immune response and the clearance of these fungal pathogens.

MATERIALS AND METHODS

Mouse strains. All mice were housed in a specific-pathogen-free facility at the Massachusetts General Hospital (MGH; Boston, MA). Inbred C57BL/6 mice were obtained from The Jackson Laboratory (Bar Harbor, ME), Dectin-1$^{-/-}$ mice were a gift from Gordon Brown (University of Aberdeen, Aberdeen, UK), and MyD88/TRIF$^{-/-}$ mice were a gift from Nir Hacohen (MGH, Boston, MA). All mice used for bone marrow harvests or *in vivo* experiments were at least 8 weeks old. Unless noted otherwise, an equal distribution of male and female mice was used. All animal experiments were approved by the Massachusetts General Hospital Institutional Animal Care and Use Committee.

Cell lines and cell culture. RAW 264.7 (RAW) macrophages were purchased from the American Type Cell Culture Collection (ATCC; Manassas, VA), C57BL/6 mouse immortalized macrophages were a gift from Douglas Golenbock (University of Massachusetts Medical School, Worcester, MA), and RAW cells expressing GFP–Dectin-1 were created as previously described (62). Primary bone marrow-derived macrophages (BMDMs) from C57BL/6, Dectin-1$^{-/-}$, and MyD88/TRIF$^{-/-}$ mice were obtained as previously described (78). All macrophages were cultured in complete RPMI 1640 medium (RPMI; L-glutamine, 10% heat-inactivated fetal bovine serum, 1% penicillin-streptomycin, 1% HEPES buffer, 50 μM 2-mercaptoethanol) or with the addition of recombinant macrophage colony-stimulating factor (for primary bone marrow-derived macrophages) and puromycin at 5 μg/ml (for GFP–Dectin-1-expressing RAW cells). All cell lines were grown at 37°C in the presence of 5% CO_2.

Fungal strains and growth. The *Exserohilum rostratum* strain used in this study was a clinical isolate obtained from the Fungus Testing Laboratory at the University of Texas Health Sciences Center in San Antonio, TX, and originated from a cerebrospinal fluid (CSF) sample recovered from a patient during the 2012 outbreak. *Exserohilum* was cultured on potato dextrose agar (Difco, Sparks, MD) and grown at room temperature. Spores were harvested in PBS–1% bovine serum albumin (BSA) after at least 1 week of growth. Spores were washed three times in PBS after collection, counted with a hemocytometer or a Luna automated cell counter (Logos Biosystems, Annandale, VA), and resuspended at the desired inoculum in PBS for cell culture stimulation experiments. For heat killing, washed *Exserohilum* spores were incubated at 95°C for 30 min. For killing by fixation, washed *Exserohilum* spores were incubated for 1 h in 4% paraformaldehyde and then washed three times in PBS, counted, and resuspended in PBS at the desired inoculum. Both methods of killing resulted in 100% killing without any observed hyphal growth after incubation for 18 h (data not shown). The spore preparations obtained were ~95% spores with some small hyphal fragments.

Confocal microscopy and analysis. For all microscopy experiments (time-lapse, differential interference contrast [DIC], and fluorescent imaging), macrophages were plated onto an 8-chambered culture cover glass (LabTek; Thermo Scientific, Rochester, NY). After stimulation, the cover glass was mounted on a Nikon Ti-E inverted microscope with a CSU-X1 confocal spinning-disk head (Yokogawa, Sugarland, TX).

The excitation source was a Coherent 4 W laser (Coherent, Santa Clara, CA), which produced excitation wavelengths of 488 and 647 nm using an acoustic optical tuner. To produce 405-nm excitation wavelengths, a UV diode laser (model BCL-050-3340; Crystal Laser LC, Reno, NV) was used. A piezo stage (Prior Instruments, Rockland, MA) capable of *x*, *y*, and *z* direction movement was used for z-stack acquisition and for imaging multiple areas of interaction during the time-lapse microscopy experiments. A polarizer (catalog number MEN 51941; Nikon) and Wollaston prisms (catalog number MBH76190; Nikon) were used to acquire DIC images. Emission light from the samples was collected after passage through the appropriate emission filters (Semrock, Rochester, NY). Images were acquired using an electron-multiplying charge-couple-device camera (catalog number C9100-13; Hamamatsu, Bridgewater, NJ). Image acquisition was performed using MetaMorph software (version 7.8.12; Molecular Devices, Downingtown, PA). Image data files were processed using Adobe Photoshop (version CS5) software and assembled in the Adobe Illustrator graphics editor (version CS5; Adobe Systems, San Jose, CA). For time-lapse microscopy, MetaMorph software was used to create videos from captured images. MetaMorph was also used to create projections from captured z-stack images.

ELISA. Macrophages were plated in 48-well tissue culture dishes at 2.5×10^5 cells per well in complete RPMI and incubated at 37°C with 5% CO_2 supplementation. Purified *Exserohilum* conidia at a multiplicity of infection (MOI) of 1:50 were added to appropriate wells. After 18 h of stimulation, the concentrations of TNF-α, IL-1β, MIP-1α, and MIP-2 in the supernatant were measured by enzyme-linked immunosorbent assay (ELISA) per the manufacturer's instructions (Duoset ELISA [R&D Systems, Minneapolis, MN] for IL-1β, MIP-1α, and MIP-2 and a BD Pharmingen [San Jose, CA] ELISA for TNF-α). When indicated, cells were incubated in the presence of voriconazole (Vfend I.V.; Novaplus) or methylprednisolone succinate (Solu-Medrol; Novaplus). For analysis of IL-1β production, the indicated macrophages were prestimulated with 500 ng/ml LPS (InvivoGen, San Diego, CA) for 4 h prior to stimulation with *Exserohilum*. Three biological replicates of each treatment condition were performed per experiment, and each experiment was performed at least three times.

Antigen staining. *Exserohilum* conidia were harvested as described above, and ~2,000 spores were inoculated into 8-well cell culture dishes containing 500 μl of complete RPMI and incubated for 0, 6, and 18 h at 37°C with 5% CO_2. At the desired time point, the plates were centrifuged at 1,000 $\times$ *g* for 5 min and the supernatants were removed and washed with PBS–1% BSA. For mannan staining, cells were incubated with fluorescein-labeled concanavalin A (ConA; catalog number C827; Invitrogen, Carlsbad, CA) for 30 min and then washed with PBS–1% BSA three times prior to confocal imaging. For β-1,3-glucan staining, cells were incubated with primary monoclonal anti-β-1,3-glucan antibody (catalog number 400-2; Biosupplies Australia Pty. Ltd., Victoria, Australia) for 30 min, washed three times with PBS–1% BSA, and then stained with secondary rabbit anti-mouse immunoglobulin conjugated with Alexa Fluor 488 (catalog number A11059; Invitrogen, Carlsbad, CA) for 30 min. Samples were again washed three times and then imaged. For chitin staining, 2 μl of calcofluor white dye (catalog number 18909; Sigma) was added to the wells, and the cells were allowed to incubate for at least 5 min prior to imaging. For galactosaminogalactan (GAG) staining, fluorescein-labeled soybean agglutinin (catalog number FL-101; Vector Laboratories, Burlingame, CA) was added to washed samples at a 1:100 dilution, and the samples were incubated for 30 min and then washed three times prior to imaging.

Dectin-1 localization. Macrophages expressing GFP–Dectin-1 were plated at 1×10^5 cells per well in an 8-well cell culture dish. *Exserohilum* conidia at an MOI of ~1:50 were added to each well. Macrophages and *Exserohilum* were cocultured for 6 or 18 h. At both time points, samples were subjected to live cell staining for chitin or fixed and stained for β-1,3-glucan. The chitin and β-1,3-glucan staining was used to visualize the *Exserohilum* hyphae for fluorescent imaging. For chitin staining, 2 μl calcofluor white dye was added directly to live cells, and the cells were incubated for at least 5 min prior to imaging. For β-1,3-glucan immunofluorescence, cultures were placed on ice and then fixed in 4% paraformaldehyde for 20 min at room temperature. After washing, they were permeabilized with 0.2% saponin for 20 min at room temperature. After incubation in blocking buffer, samples were incubated with primary anti-β-1,3-glucan antibody for 1 h, washed, and then incubated with secondary rabbit anti-mouse immunoglobulin conjugated with Alexa Fluor 647 (catalog number A21239; Invitrogen, Carlsbad, CA) for 1 h. After washing, the cells were imaged by confocal microscopy.

Hyphal mass assay. The hyphal mass assay method used in this study was adapted from hyphal mass assays published for *Aspergillus fumigatus* (66). Macrophages (2.5×10^5) were stimulated with *Exserohilum* at an MOI of 1:50 in 48-well cell culture plates for 18 h at 37°C. At that time, the plates were centrifuged at 1,000 $\times$ *g* for 5 min and the supernatants were carefully removed. A 1:5 dilution of calcofluor white stain in distilled H_2O was added to each well, and the plates were incubated for 20 min in the dark. The wells were then washed three times with H_2O, and samples were resuspended in 400 μl of H_2O. Fluorescence was measured using a SpectraMax i3x multimode microplate reader (Molecular Devices, Sunnyvale, CA) at an excitation wavelength of 360 nm and an absorbance of 440 nm. Five biological replicates were performed for each treatment condition per experiment, and each experiment was repeated at least three times. The results are reported as the relative fluorescence, which is the average fluorescence obtained for each treatment condition minus the average background fluorescence (the fluorescence of macrophages alone, without addition of *Exserohilum*).

Soft tissue infection model. The protocol for the soft tissue infection model was adapted from published soft tissue infection models used for *Aspergillus fumigatus* (10). *Exserohilum* spores were harvested in PBS–0.008% Tween and washed three times in PBS–0.008% Tween. Spores were diluted to 2×10^5 spores in 120 μl of PBS–0.008% Tween or 120 μl of PBS–0.008% Tween containing 13 mg/ml of methylprednisolone acetate (MPA; Depo-Medrol; Novaplus).

Mice were anesthetized using isoflurane. The posterior flanks and upper thighs of C57BL/6 mice were shaved using a Philips Norelco trimmer (model Multigroom 3100; Stamford, CT). *Exserohilum* was injected subcutaneously into the right upper thigh of the mice, while a paired control treatment consisting of vehicle alone was injected into the left upper thigh. Mice were observed daily and euthanized on day 10. There were a total of five mice per treatment group. Soft tissue encompassing the area of inflammation or the initial injection site was excised and fixed in 10% formalin. The tissue was further processed and paraffin embedded at the MGH Histopathology Research Core. Tissue was stained with the hematoxylin and eosin (H&E) and Grocott's methenamine silver (GMS) stains (Polysciences, Inc., Warrington, PA). Tissue samples were reviewed blind by a pathologist at the MGH Histopathology Research Core.

Statistics. For the ELISA and the hyphal mass assays, statistics were performed using GraphPad Prism (version 6) software. Statistical analyses were performed using one-way analysis of variance (ANOVA) with Tukey posttests or two-way ANOVA, as indicated in the figure legends. Graphs depict the means, with error bars denoting the standard errors of the means (SEMs) from at least three biological replicates for each treatment condition. Each experiment was repeated at least three times, and the results from a representative experiment are shown. For spore localization experiments, statistical analyses were performed using GraphPad Prism (version 6) software and chi-square testing. Data were considered significantly different if the P value was <0.05.

SUPPLEMENTAL MATERIAL

Supplemental material for this article may be found at https://doi.org/10.1128/IAI.00903-16.

TEXT S1, PDF file, 0.3 MB.

VIDEO S1, MOV file, 13.7 MB.

ACKNOWLEDGMENTS

We thank the MGH Infectious Diseases Division for support.

We are grateful to a patient of J.M.V. who provided unrestricted funds that were used in part to support this study. J.L.R. was supported by a KL2/Catalyst Medical Research Investigator Training award (an appointed KL2 award) from Harvard Catalyst | The Harvard Clinical and Translational Science Center (National Center for Research Resources and the National Center for Advancing Translational Sciences, National Institutes of Health [NIH], award KL2 TR001100), and NIH grant T32 AI007061. J.M.V. was supported by National Institutes of Health grants 5R01 AI092084 and 5R21 AI109303. M.K.M. was supported by NIH/NIAID grant 1K08 AI110655.

The content is solely the responsibility of the authors and does not necessarily represent the official views of Harvard Catalyst, Harvard University and its affiliated academic health care centers, or the National Institutes of Health.

J.L.R. performed the experiments, designed the research studies, analyzed the data, and wrote the manuscript. P.E.N. assisted with the performance of the experiments and acquisition of the data, particularly those from the ELISA and hyphal mass assays. T.F.P. and N.P.W. contributed the fungal strains and contributed to critical evaluation of the manuscript. M.F. managed all mice for the laboratory and assisted with the *in vivo* experiments. N.S.K., J.M.T., M.K.M., and D.P.L. all assisted with the design of the research studies and provided reagents and technical microscopy expertise. J.M.V. assisted with the design of the research studies and analysis of the data, provided reagents, and assisted with the writing of the manuscript.

REFERENCES

1. Revankar SG. 2007. Dematiaceous fungi. Mycoses 50:91–101. https://doi.org/10.1111/j.1439-0507.2006.01331.x.
2. Pappas PG, Alexander BD, Andes DR, Hadley S, Kauffman CA, Freifeld A, Anaissie EJ, Brumble LM, Herwaldt L, Ito J, Kontoyiannis DP, Lyon GM, Marr KA, Morrison VA, Park BJ, Patterson TF, Perl TM, Oster RA, Schuster MG, Walker R, Walsh TJ, Wannemuehler KA, Chiller TM. 2010. Invasive fungal infections among organ transplant recipients: results of the Transplant-Associated Infection Surveillance Network (TRANSNET). Clin Infect Dis 50:1101–1111. https://doi.org/10.1086/651262.
3. Kontoyiannis DP, Marr KA, Park BJ, Alexander BD, Anaissie EJ, Walsh TJ, Ito J, Andes DR, Baddley JW, Brown JM, Brumble LM, Freifeld AG, Hadley S, Herwaldt LA, Kauffman CA, Knapp K, Lyon GM, Morrison VA, Papanicolaou G, Patterson TF, Perl TM, Schuster MG, Walker R, Wannemuehler KA, Wingard JR, Chiller TM, Pappas PG. 2010. Prospective surveillance for invasive fungal infections in hematopoietic stem cell transplant recipients, 2001–2006: overview of the Transplant-Associated Infection Surveillance Network (TRANSNET) Database. Clin Infect Dis 50:1091–1100. https://doi.org/10.1086/651263.
4. Lyons JL, Gireesh ED, Trivedi JB, Bell WR, Cettomai D, Smith BR, Karram S, Chang T, Tochen L, Zhang SX, McCall CM, Pearce DT, Carroll KC, Chen L, Ratchford JN, Harrison DM, Ostrow LW, Stevens RD. 2012. Fatal Exserohilum meningitis and central nervous system vasculitis after cervical epidural methylprednisolone injection. Ann Intern Med 157:835–836. https://doi.org/10.7326/0003-4819-158-1-201212040-00557.
5. CDC. 2016. Multistate outbreak of fungal meningitis and other infections–case count. CDC, Atlanta, GA. https://www.cdc.gov/hai/outbreaks/meningitis-map-large.html#casecount_table. Accessed 25 September 2016.

6. Smith RM, Tipple M, Chaudry MN, Schaefer MK, Park BJ. 2013. Relapse of fungal meningitis associated with contaminated methylprednisolone. N Engl J Med 368:2535–2536. https://doi.org/10.1056/NEJMc1306560.
7. Terry AR, Kahle KT, Larvie M, Vyas JM, Stemmer-Rachamimov A. 2016. Case records of the Massachusetts General Hospital. Case 5-2016. A 43-year-old man with altered mental status and a history of alcohol use. N Engl J Med 374:671–680. https://doi.org/10.1056/NEJMcpc1509361.
8. Latge JP. 2010. Tasting the fungal cell wall. Cell Microbiol 12:863–872. https://doi.org/10.1111/j.1462-5822.2010.01474.x.
9. Romani L. 2011. Immunity to fungal infections. Nat Rev Immunol 11:275–288. https://doi.org/10.1038/nri2939.
10. Carrion SDJ, Leal SM, Jr, Ghannoum MA, Aimanianda V, Latge JP, Pearlman E. 2013. The RodA hydrophobin on Aspergillus fumigatus spores masks dectin-1- and dectin-2-dependent responses and enhances fungal survival in vivo. J Immunol 191:2581–2588. https://doi.org/10.4049/jimmunol.1300748.
11. Dague E, Alsteens D, Latge JP, Dufrene YF. 2008. High-resolution cell surface dynamics of germinating Aspergillus fumigatus conidia. Biophys J 94:656–660. https://doi.org/10.1529/biophysj.107.116491.
12. Girardin H, Paris S, Rault J, Bellon-Fontaine MN, Latge JP. 1999. The role of the rodlet structure on the physicochemical properties of Aspergillus conidia. Lett Appl Microbiol 29:364–369. https://doi.org/10.1046/j.1472-765X.1999.00643.x.
13. Botts MR, Giles SS, Gates MA, Kozel TR, Hull CM. 2009. Isolation and characterization of Cryptococcus neoformans spores reveal a critical role for capsule biosynthesis genes in spore biogenesis. Eukaryot Cell 8:595–605. https://doi.org/10.1128/EC.00352-08.
14. Giles SS, Dagenais TR, Botts MR, Keller NP, Hull CM. 2009. Elucidating the pathogenesis of spores from the human fungal pathogen Cryptococcus neoformans. Infect Immun 77:3491–3500. https://doi.org/10.1128/IAI.00334-09.
15. Cross CE, Bancroft GJ. 1995. Ingestion of acapsular Cryptococcus neoformans occurs via mannose and beta-glucan receptors, resulting in cytokine production and increased phagocytosis of the encapsulated form. Infect Immun 63:2604–2611.
16. Panepinto JC, Komperda KW, Hacham M, Shin S, Liu X, Williamson PR. 2007. Binding of serum mannan binding lectin to a cell integrity-defective Cryptococcus neoformans ccr4Δ mutant. Infect Immun 75:4769–4779. https://doi.org/10.1128/IAI.00536-07.
17. Domer JE, Garner RE, Befidi-Mengue RN. 1989. Mannan as an antigen in cell-mediated immunity (CMI) assays and as a modulator of mannan-specific CMI. Infect Immun 57:693–700.
18. Domer JE, Stashak PW, Elkins K, Prescott B, Caldes G, Baker PJ. 1986. Separation of immunomodulatory effects of mannan from Candida albicans into stimulatory and suppressive components. Cell Immunol 101:403–414. https://doi.org/10.1016/0008-8749(86)90153-X.
19. Netea MG, Gow NA, Munro CA, Bates S, Collins C, Ferwerda G, Hobson RP, Bertram G, Hughes HB, Jansen T, Jacobs L, Buurman ET, Gijzen K, Williams DL, Torensma R, McKinnon A, MacCallum DM, Odds FC, Van der Meer JW, Brown AJ, Kullberg BJ. 2006. Immune sensing of Candida albicans requires cooperative recognition of mannans and glucans by lectin and Toll-like receptors. J Clin Invest 116:1642–1650. https://doi.org/10.1172/JCI27114.
20. Paulovicova L, Paulovicova E, Karelin AA, Tsvetkov YE, Nifantiev NE, Bystricky S. 2015. Immune cell response to Candida cell wall mannan derived branched alpha-oligomannoside conjugates in mice. J Microbiol Immunol Infect 48:9–19. https://doi.org/10.1016/j.jmii.2013.08.020.
21. Suzuki I, Hashimoto K, Yadomae T. 1988. The effects of a highly branched beta-1,3-glucan, SSG, obtained from Sclerotinia sclerotiorum IFO 9395 on the growth of syngeneic tumors in mice. J Pharmacobiodyn 11:527–532. https://doi.org/10.1248/bpb1978.11.527.
22. Sakurai T, Ohno N, Yadomae T. 1994. Changes in immune mediators in mouse lung produced by administration of soluble (1 → 3)-beta-D-glucan. Biol Pharm Bull 17:617–622. https://doi.org/10.1248/bpb.17.617.
23. Williams DL. 1997. Overview of (1 → 3)-beta-D-glucan immunobiology. Mediators Inflamm 6:247–250. https://doi.org/10.1080/09629359791550.
24. Miura T, Ohno N, Miura NN, Adachi Y, Shimada S, Yadomae T. 1999. Antigen-specific response of murine immune system toward a yeast beta-glucan preparation, zymosan. FEMS Immunol Med Microbiol 24:131–139.
25. Lee JN, Lee DY, Ji IH, Kim GE, Kim HN, Sohn J, Kim S, Kim CW. 2001. Purification of soluble beta-glucan with immune-enhancing activity from the cell wall of yeast. Biosci Biotechnol Biochem 65:837–841. https://doi.org/10.1271/bbb.65.837.
26. Pelizon AC, Kaneno R, Soares AM, Meira DA, Sartori A. 2003. Down-modulation of lymphoproliferation and interferon-gamma production by beta-glucan derived from Saccharomyces cerevisiae. Mem Inst Oswaldo Cruz 98:1083–1087. https://doi.org/10.1590/S0074-02762003000800019.
27. Hohl TM, Van Epps HL, Rivera A, Morgan LA, Chen PL, Feldmesser M, Pamer EG. 2005. Aspergillus fumigatus triggers inflammatory responses by stage-specific beta-glucan display. PLoS Pathog 1:e30. https://doi.org/10.1371/journal.ppat.0010030.
28. Li J, Xing J, Li D, Wang X, Zhao L, Lv S, Huang D. 2005. Effects of beta-glucan extracted from Saccharomyces cerevisiae on humoral and cellular immunity in weaned piglets. Arch Anim Nutr 59:303–312. https://doi.org/10.1080/17450390500247832.
29. Luther K, Torosantucci A, Brakhage AA, Heesemann J, Ebel F. 2007. Phagocytosis of Aspergillus fumigatus conidia by murine macrophages involves recognition by the Dectin-1 beta-glucan receptor and Toll-like receptor 2. Cell Microbiol 9:368–381. https://doi.org/10.1111/j.1462-5822.2006.00796.x.
30. Noss I, Ozment TR, Graves BM, Kruppa MD, Rice PJ, Williams DL. 2015. Cellular and molecular mechanisms of fungal beta-(1 → 6)-glucan in macrophages. Innate Immun 21:759–769. https://doi.org/10.1177/1753425915595874.
31. Fontaine T, Delangle A, Simenel C, Coddeville B, van Vliet SJ, van Kooyk Y, Bozza S, Moretti S, Schwarz F, Trichot C, Aebi M, Delepierre M, Elbim C, Romani L, Latge JP. 2011. Galactosaminogalactan, a new immunosuppressive polysaccharide of Aspergillus fumigatus. PLoS Pathog 7:e1002372. https://doi.org/10.1371/journal.ppat.1002372.
32. Gravelat FN, Beauvais A, Liu H, Lee MJ, Snarr BD, Chen D, Xu W, Kravtsov I, Hoareau CM, Vanier G, Urb M, Campoli P, Al Abdallah Q, Lehoux M, Chabot JC, Ouimet MC, Baptista SD, Fritz JH, Nierman WC, Latge JP, Mitchell AP, Filler SG, Fontaine T, Sheppard DC. 2013. Aspergillus galactosaminogalactan mediates adherence to host constituents and conceals hyphal beta-glucan from the immune system. PLoS Pathog 9:e1003575. https://doi.org/10.1371/journal.ppat.1003575.
33. Gresnigt MS, Bozza S, Becker KL, Joosten LA, Abdollahi-Roodsaz S, van der Berg WB, Dinarello CA, Netea MG, Fontaine T, De Luca A, Moretti S, Romani L, Latge JP, van de Veerdonk FL. 2014. A polysaccharide virulence factor from Aspergillus fumigatus elicits anti-inflammatory effects through induction of interleukin-1 receptor antagonist. PLoS Pathog 10:e1003936. https://doi.org/10.1371/journal.ppat.1003936.
34. Robinet P, Baychelier F, Fontaine T, Picard C, Debre P, Vieillard V, Latge JP, Elbim C. 2014. A polysaccharide virulence factor of a human fungal pathogen induces neutrophil apoptosis via NK cells. J Immunol 192:5332–5342. https://doi.org/10.4049/jimmunol.1303180.
35. Lee MJ, Liu H, Barker BM, Snarr BD, Gravelat FN, Al Abdallah Q, Gavino C, Baistrocchi SR, Ostapska H, Xiao T, Ralph B, Solis NV, Lehoux M, Baptista SD, Thammahong A, Cerone RP, Kaminskyj SG, Guiot MC, Latge JP, Fontaine T, Vinh DC, Filler SG, Sheppard DC. 2015. The fungal exopolysaccharide galactosaminogalactan mediates virulence by enhancing resistance to neutrophil extracellular traps. PLoS Pathog 11:e1005187. https://doi.org/10.1371/journal.ppat.1005187.
36. Henriet SS, van de Sande WW, Lee MJ, Simonetti E, Momany M, Verweij PE, Rijs AJ, Ferwerda G, Sheppard DC, de Jonge MI, Warris A. 2016. Decreased cell wall galactosaminogalactan in Aspergillus nidulans mediates dysregulated inflammation in the chronic granulomatous disease host. J Interferon Cytokine Res 36:488–498. https://doi.org/10.1089/jir.2015.0095.
37. Reese TA, Liang HE, Tager AM, Luster AD, Van Rooijen N, Voehringer D, Locksley RM. 2007. Chitin induces accumulation in tissue of innate immune cells associated with allergy. Nature 447:92–96. https://doi.org/10.1038/nature05746.
38. Da Silva CA, Hartl D, Liu W, Lee CG, Elias JA. 2008. TLR-2 and IL-17A in chitin-induced macrophage activation and acute inflammation. J Immunol 181:4279–4286. https://doi.org/10.4049/jimmunol.181.6.4279.
39. Lee CG, Da Silva CA, Lee JY, Hartl D, Elias JA. 2008. Chitin regulation of immune responses: an old molecule with new roles. Curr Opin Immunol 20:684–689. https://doi.org/10.1016/j.coi.2008.10.002.
40. Wagner CJ, Huber S, Wirth S, Voehringer D. 2010. Chitin induces up-regulation of B7-H1 on macrophages and inhibits T-cell proliferation. Eur J Immunol 40:2882–2890. https://doi.org/10.1002/eji.201040422.
41. Mora-Montes HM, Netea MG, Ferwerda G, Lenardon MD, Brown GD, Mistry AR, Kullberg BJ, O'Callaghan CA, Sheth CC, Odds FC, Brown AJ, Munro CA, Gow NA. 2011. Recognition and blocking of innate immunity

cells by Candida albicans chitin. Infect Immun 79:1961–1970. https://doi.org/10.1128/IAI.01282-10.
42. Dubey LK, Moeller JB, Schlosser A, Sorensen GL, Holmskov U. 2014. Induction of innate immunity by Aspergillus fumigatus cell wall polysaccharides is enhanced by the composite presentation of chitin and beta-glucan. Immunobiology 219:179–188. https://doi.org/10.1016/j.imbio.2013.10.003.
43. Wagener J, Malireddi RK, Lenardon MD, Koberle M, Vautier S, MacCallum DM, Biedermann T, Schaller M, Netea MG, Kanneganti TD, Brown GD, Brown AJ, Gow NA. 2014. Fungal chitin dampens inflammation through IL-10 induction mediated by NOD2 and TLR9 activation. PLoS Pathog 10:e1004050. https://doi.org/10.1371/journal.ppat.1004050.
44. Amarsaikhan N, Templeton SP. 2015. Co-recognition of beta-glucan and chitin and programming of adaptive immunity to Aspergillus fumigatus. Front Microbiol 6:344. https://doi.org/10.3389/fmicb.2015.00344.
45. Rizzetto L, Ifrim DC, Moretti S, Tocci N, Cheng SC, Quintin J, Renga G, Oikonomou V, De Filippo C, Weil T, Blok BA, Lenucci MS, Santos MA, Romani L, Netea MG, Cavalieri D. 2016. Fungal chitin induces trained immunity in human monocytes during cross-talk of the host with Saccharomyces cerevisiae. J Biol Chem 291:7961–7972. https://doi.org/10.1074/jbc.M115.699645.
46. Kasperkovitz PV, Khan NS, Tam JM, Mansour MK, Davids PJ, Vyas JM. 2011. Toll-like receptor 9 modulates macrophage antifungal effector function during innate recognition of Candida albicans and Saccharomyces cerevisiae. Infect Immun 79:4858–4867. https://doi.org/10.1128/IAI.05626-11.
47. Gow NA, Netea MG, Munro CA, Ferwerda G, Bates S, Mora-Montes HM, Walker L, Jansen T, Jacobs L, Tsoni V, Brown GD, Odds FC, Van der Meer JW, Brown AJ, Kullberg BJ. 2007. Immune recognition of Candida albicans beta-glucan by dectin-1. J Infect Dis 196:1565–1571. https://doi.org/10.1086/523110.
48. Gantner BN, Simmons RM, Underhill DM. 2005. Dectin-1 mediates macrophage recognition of Candida albicans yeast but not filaments. EMBO J 24:1277–1286. https://doi.org/10.1038/sj.emboj.7600594.
49. Brown GD, Taylor PR, Reid DM, Willment JA, Williams DL, Martinez-Pomares L, Wong SY, Gordon S. 2002. Dectin-1 is a major beta-glucan receptor on macrophages. J Exp Med 196:407–412. https://doi.org/10.1084/jem.20020470.
50. Taylor PR, Brown GD, Reid DM, Willment JA, Martinez-Pomares L, Gordon S, Wong SY. 2002. The beta-glucan receptor, dectin-1, is predominantly expressed on the surface of cells of the monocyte/macrophage and neutrophil lineages. J Immunol 169:3876–3882. https://doi.org/10.4049/jimmunol.169.7.3876.
51. Taylor PR, Tsoni SV, Willment JA, Dennehy KM, Rosas M, Findon H, Haynes K, Steele C, Botto M, Gordon S, Brown GD. 2007. Dectin-1 is required for beta-glucan recognition and control of fungal infection. Nat Immunol 8:31–38. https://doi.org/10.1038/ni1408.
52. Gantner BN, Simmons RM, Canavera SJ, Akira S, Underhill DM. 2003. Collaborative induction of inflammatory responses by dectin-1 and Toll-like receptor 2. J Exp Med 197:1107–1117. https://doi.org/10.1084/jem.20021787.
53. Gersuk GM, Underhill DM, Zhu L, Marr KA. 2006. Dectin-1 and TLRs permit macrophages to distinguish between different Aspergillus fumigatus cellular states. J Immunol 176:3717–3724. https://doi.org/10.4049/jimmunol.176.6.3717.
54. Underhill DM. 2007. Collaboration between the innate immune receptors dectin-1, TLRs, and Nods. Immunol Rev 219:75–87. https://doi.org/10.1111/j.1600-065X.2007.00548.x.
55. Goodridge HS, Underhill DM. 2008. Fungal recognition by TLR2 and Dectin-1. Handb Exp Pharmacol 5:87–109. https://doi.org/10.1007/978-3-540-72167-3_5.
56. Calich VL, Pina A, Felonato M, Bernardino S, Costa TA, Loures FV. 2008. Toll-like receptors and fungal infections: the role of TLR2, TLR4 and MyD88 in paracoccidioidomycosis. FEMS Immunol Med Microbiol 53:1–7. https://doi.org/10.1111/j.1574-695X.2008.00378.x.
57. Blasi E, Mucci A, Neglia R, Pezzini F, Colombari B, Radzioch D, Cossarizza A, Lugli E, Volpini G, Del Giudice G, Peppoloni S. 2005. Biological importance of the two Toll-like receptors, TLR2 and TLR4, in macrophage response to infection with Candida albicans. FEMS Immunol Med Microbiol 44:69–79. https://doi.org/10.1016/j.femsim.2004.12.005.
58. Yamamoto M, Sato S, Hemmi H, Hoshino K, Kaisho T, Sanjo H, Takeuchi O, Sugiyama M, Okabe M, Takeda K, Akira S. 2003. Role of adaptor TRIF in the MyD88-independent Toll-like receptor signaling pathway. Science 301:640–643. https://doi.org/10.1126/science.1087262.
59. Netea MG, Nold-Petry CA, Nold MF, Joosten LA, Opitz B, van der Meer JH, van de Veerdonk FL, Ferwerda G, Heinhuis B, Devesa I, Funk CJ, Mason RJ, Kullberg BJ, Rubartelli A, van der Meer JW, Dinarello CA. 2009. Differential requirement for the activation of the inflammasome for processing and release of IL-1beta in monocytes and macrophages. Blood 113:2324–2335. https://doi.org/10.1182/blood-2008-03-146720.
60. Netea MG, Simon A, van de Veerdonk F, Kullberg BJ, Van der Meer JW, Joosten LA. 2010. IL-1beta processing in host defense: beyond the inflammasomes. PLoS Pathog 6:e1000661. https://doi.org/10.1371/journal.ppat.1000661.
61. Steele C, Rapaka RR, Metz A, Pop SM, Williams DL, Gordon S, Kolls JK, Brown GD. 2005. The beta-glucan receptor dectin-1 recognizes specific morphologies of Aspergillus fumigatus. PLoS Pathog 1:e42. https://doi.org/10.1371/journal.ppat.0010042.
62. Mansour MK, Tam JM, Khan NS, Seward M, Davids PJ, Puranam S, Sokolovska A, Sykes DB, Dagher Z, Becker C, Tanne A, Reedy JL, Stuart LM, Vyas JM. 2013. Dectin-1 activation controls maturation of beta-1,3-glucan-containing phagosomes. J Biol Chem 288:16043–16054. https://doi.org/10.1074/jbc.M113.473223.
63. Pappas PG, Kontoyiannis DP, Perfect JR, Chiller TM. 2013. Real-time treatment guidelines: considerations during the Exserohilum rostratum outbreak in the United States. Antimicrob Agents Chemother 57:1573–1576. https://doi.org/10.1128/AAC.00205-13.
64. Stevens DA. 2013. Reflections on the approach to treatment of a mycologic disaster. Antimicrob Agents Chemother 57:1567–1572. https://doi.org/10.1128/AAC.02242-12.
65. da Cunha KC, Sutton DA, Gene J, Capilla J, Cano J, Guarro J. 2012. Molecular identification and in vitro response to antifungal drugs of clinical isolates of Exserohilum. Antimicrob Agents Chemother 56:4951–4954. https://doi.org/10.1128/AAC.00488-12.
66. Leal SM, Jr, Roy S, Vareechon C, Carrion S, Clark H, Lopez-Berges MS, Di Pietro A, Schrettl M, Beckmann N, Redl B, Haas H, Pearlman E. 2013. Targeting iron acquisition blocks infection with the fungal pathogens Aspergillus fumigatus and Fusarium oxysporum. PLoS Pathog 9:e1003436. https://doi.org/10.1371/journal.ppat.1003436.
67. Farmakiotis D, Shirazi F, Zhao Y, Saad PJ, Albert ND, Roilides E, Walsh TJ, Perlin DS, Kontoyiannis DP. 2014. Methylprednisolone enhances the growth of Exserohilum rostratum in vitro, attenuates spontaneous apoptosis, and increases mortality rates in immunocompetent Drosophila flies. J Infect Dis 210:1471–1475. https://doi.org/10.1093/infdis/jiu289.
68. Katragkou A, Pana ZD, Perlin DS, Kontoyiannis DP, Walsh TJ, Roilides E. 2014. Exserohilum infections: review of 48 cases before the 2012 United States outbreak. Med Mycol 52:376–386. https://doi.org/10.1093/mmy/myt030.
69. Ritter JM, Muehlenbachs A, Blau DM, Paddock CD, Shieh WJ, Drew CP, Batten BC, Bartlett JH, Metcalfe MG, Pham CD, Lockhart SR, Patel M, Liu L, Jones TL, Greer PW, Montague JL, White E, Rollin DC, Seales C, Stewart D, Deming MV, Brandt ME, Zaki SR, Exserohilum Infections Working Group. 2013. Exserohilum infections associated with contaminated steroid injections: a clinicopathologic review of 40 cases. Am J Pathol 183:881–892. https://doi.org/10.1016/j.ajpath.2013.05.007.
70. Rappleye CA, Eissenberg LG, Goldman WE. 2007. Histoplasma capsulatum alpha-(1,3)-glucan blocks innate immune recognition by the beta-glucan receptor. Proc Natl Acad Sci U S A 104:1366–1370. https://doi.org/10.1073/pnas.0609848104.
71. Rosas M, Liddiard K, Kimberg M, Faro-Trindade I, McDonald JU, Williams DL, Brown GD, Taylor PR. 2008. The induction of inflammation by Dectin-1 in vivo is dependent on myeloid cell programming and the progression of phagocytosis. J Immunol 181:3549–3557. https://doi.org/10.4049/jimmunol.181.5.3549.
72. Hernanz-Falcon P, Joffre O, Williams DL, Reis e, Sousa C. 2009. Internalization of Dectin-1 terminates induction of inflammatory responses. Eur J Immunol 39:507–513. https://doi.org/10.1002/eji.200838687.
73. Taylor PR, Roy S, Leal SM, Jr, Sun Y, Howell SJ, Cobb BA, Li X, Pearlman E. 2014. Activation of neutrophils by autocrine IL-17A-IL-17RC interactions during fungal infection is regulated by IL-6, IL-23, RORγt and Dectin-2. Nat Immunol 15:143–151. https://doi.org/10.1038/ni.2797.
74. Jhingran A, Mar KB, Kumasaka DK, Knoblaugh SE, Ngo LY, Segal BH, Iwakura Y, Lowell CA, Hamerman JA, Lin X, Hohl TM. 2012. Tracing conidial fate and measuring host cell antifungal activity using a reporter of microbial viability in the lung. Cell Rep 2:1762–1773. https://doi.org/10.1016/j.celrep.2012.10.026.
75. Wang X, Wang W, Lin Z, Wang X, Li T, Yu J, Liu W, Tong Z, Xu Y, Zhang J, Guan L, Dai L, Yang Y, Han W, Li R. 2014. CARD9 mutations linked to

subcutaneous phaeohyphomycosis and TH17 cell deficiencies. J Allergy Clin Immunol 133:905–908.e3. https://doi.org/10.1016/j.jaci.2013.09.033.
76. Wu W, Zhang R, Wang X, Song Y, Liu Z, Han W, Li R. 2016. Impairment of immune response against dematiaceous fungi in Card9 knockout mice. Mycopathologia 181:631–642. https://doi.org/10.1007/s11046-016-0029-0.
77. Simitsopoulou M, Walsh TJ, Kyrpitzi D, Petraitis V, Kontoyiannis DP, Perlin DS, Roilides E. 2015. Methylprednisolone impairs conidial phagocytosis but does not attenuate hyphal damage by neutrophils against Exserohilum rostratum. Med Mycol 53:189–193. https://doi.org/10.1093/mmy/myu034.
78. Tam JM, Mansour MK, Khan NS, Seward M, Puranam S, Tanne A, Sokolovska A, Becker CE, Acharya M, Baird MA, Choi AM, Davidson MW, Segal BH, Lacy-Hulbert A, Stuart LM, Xavier RJ, Vyas JM. 2014. Dectin-1-dependent LC3 recruitment to phagosomes enhances fungicidal activity in macrophages. J Infect Dis 210:1844–1854. https://doi.org/10.1093/infdis/jiu290.